Combined multidimensional approaches for the simulation of flow trough a wall-flow particulate filter

A. N. Impiombato[1] G.Discepoli[1] F. Paltrinieri[1] M. Milano[2] L. Montorsi [2]

luca.montorsi@unimore.it

https://orcid.org/0000-0002-4910-5693

[1]Department of Science and Methods for Engineering,
University of Modena and Reggio Emilia 42121 Reggio Emilia, Italy

[2]Department of Science and Methods for Engineering-Centro En&Tech
University of Modena and Reggio Emilia 42121 Reggio Emilia, Italy

Abstract.

The paper proposes a combined CFD and 1D approach for the numerical analysis of porous media typical of particulates filters. Due to the geometric complexity of the filter, the model combined the CFD flow simulation upstream the porous medium with the lumped and distributed parameter simulation of the elemental cells of the porous medium. The proposed mathematical model for solving the flow within the porous medium considers the exhaust gas flow within a single three-dimensional trap cell taking continuity and momentum balance into account. The non-linear set of equations of the elements encompassing the porous medium are solved numerically using a one-dimensional approach and combined iteratively with the CFD solution. The pressure drop due to the crossing of the elemental cell walls composed by the particulate layer and the porous medium is modeled using the Darcy's law. The predictive capabilities of the proposed numerical approach are addressed by comparing the numerical results of the model with the data available in literature for a reference geometry

.**Keywords**. Computational Fluid Dynamics, Star CCM+, Particulate Filter, Porous Media, Pressure Drop

1. INTRODUCTION

The exhaust gases generated by the internal combustion engines are among the main causes of pollution as they carry out in the form of aerosols quantities of pollutants harmful to the environment and human health [1], [2]. To lower the pollutants level, automotive companies, in addition to various control systems on the quality of engine combustion, adopt exhaust fumes filtering systems [3]. A Broad field of research is also carried out on the development

of fully sustainable vehicles (such as innovative electric buses [4] or solar-powered vehicles for [5], [6]).

The most commonly used filter is the one with wall-flow geometry, in which the exhaust gases are forced to pass between the filter cells and throughout the porous matrix that separates the different cells. Obviously, the insertion of the monolith in the flue gas exhaust duct produces a pressure drop that the engine has to perform a higher job to ensure that the fumes overcome it. This affects the engine performance, especially the fuel efficiency. Therefore, the ability to accurately predict the back pressure caused by the filter monolith has become very important for automotive companies in optic to optimizing their vehicles [7].

The first fundamental study on the regenerative process of the filter was proposed by Bisset [8] in 1984; the author proposes a one-dimensional model of mass balance, momentum and energy equations. This work was the starting point of subsequent works which had the purpose of predicting the pressure drop in different working conditions. Prantoni et al. [9] adopted the Bisset model [8] in the hypothesis of fluid dynamic interaction between the cells that make up the entire wall-flow filter. While Aleksandrova et al. [10] used the Bissett model [8] to characterize particulate filters for diesel and gasoline engines under different flow conditions but at a fixed temperature. Furthermore, Koltsakis et al. [11] and Yang et al. [12] report further examples of application of the Bissett model [8] for the characterization of particulate filters. In a previous work [13] the dimensionless model of the filter for determining the pressure drop was obtained. Most of these models are based on a scaling approach so that the filter pressure drop can be modeled considering a simplified geometry that includes a single inlet and outlet channel. According with the literature ([7], [9], [13]), the approximation introduced by the scaling approach can be justified when the velocity profile entering the filter is constant so that the mass flow rate is the same in all channels, and when the ratio between the hydraulic diameter of the cell and the filter diameter is very small ($d / D_{filter} << 1$). In other words, the full coupling between open and closed channels is negligible on the scale of the entire filter. It is worth mentioning that the applicability of the scaling approach is also limited to filters with homogeneous properties, i.e. all the cells have the same hydraulic diameter, all the porous walls have the same permeability, and soot is distributed homogeneously.

Depending on how the soot is deposited inside the filter cells, the efficiency of the filter also changes. Simulating the filter in this scenario requires the modeling of the interaction events between particles and the porous matrix (Lattice-Boltzmann method), with a high computational cost ([14]–[16]). Another problem that affects the simulation of a real porous medium is the modelling of geometry. On this regard,

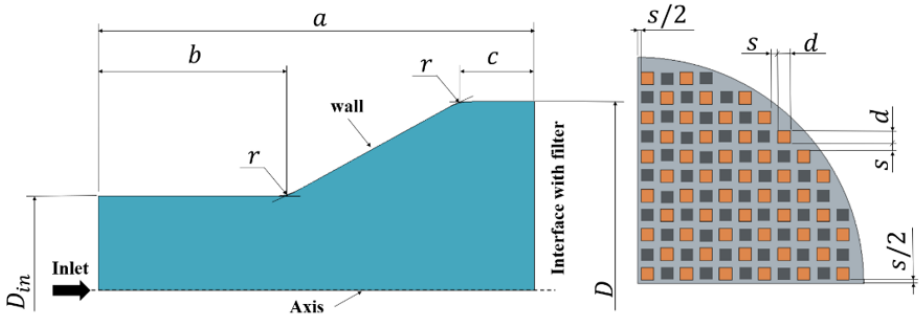

Symbol	D_{in}	D	a	b	c	r	s	d
Value	25.00	50.00	50	25	10	5	0.76	1.40
Unit	mm	mm	mm	mm	mm	mm	mm	mm

Figure.1. CFD computational domain (left); frontal view (right): the open cells are coloured in orange and the closed cells are coloured in black. Geometry measure (bottom).

some authors used the Voronoi tessellation (as reported in [17], [18]), while others used real images obtained from an X-ray [19].

This work analyzes how the fluid dynamics upstream of the filter is influenced inside the duct considering the entire geometry of the monolith. To do this the Computational Fluid Dynamics (CFD) was used to determine the flow field before the monolith and, once the inlet velocity conditions to the individual cells have been obtained, an external code was used to obtain the pressure value in the individual faces of the cells in which the fluid enters. To arrive at the final solution, an iterative process was established between the CFD software and the external code. It is important to specify that, in this work, an ideal gas maintained at fixed temperature of *953.15 K* was considered and no model is used to describe the particulate matter. The results show that the pressure distribution upstream of the filter is not uniform and this affects the velocity range in a way that is not easily predictable.

2. CFD MODEL

In order to demonstrate the coupling between the CFD simulation and the code for solving the governing equations inside the filter channels, the pipe is described in Fig.1. Only the open cells (orange) represent the outlet sections from the fluid domain (i.e. entering the filter). The closed cells (black), on the other hand, have been shown for the sake of clarity, but they are not part of the CFD domain. These, together with the gray part of Fig.1, are seen as a single wall. This assumption is a simplification, as in reality the closed cells (black) are obstructed by a plug. This assumption does not affect the final result as Prantoni M, et al. [9] demonstrated. The geometrical symmetry along the axis permits to consider only a quarter of the entire physical domain, this resulting in a lower computational cost, thus without any loss of information.

In the fluid domain, the Standard k-ω turbulence model [20] (an explanation of the model is provided in Appendix A) was solved using Star-CCM+ [21] considering the set-up of Tab.1.

A velocity inlet of 1 m/s of hot air gas was prescribed at the geometry inlet section. The filter is not included in the computational domain, but the entrance faces of the inlet channels are included (orange cells in Fig.1) and set up as pressure outlets. The value of the pressure for each channel is

Table 1. StarCCM+ set-up parameters

Parameter	**Model**
Domain	3-D
Time	Steady state
Flow solver	Segregated flow
Viscous regime	Turbulent
Model	*k-ω*
Temperature	Isothermal, *T=953.15 K*
Equation of state	Ideal gas law
Fluid	Air
Viscosity	Sutherland's law

determined from the multi-channel model and is discussed in the next section. The remaining boundary surfaces are set-up as no slip walls.

As shown in Fig.2, a polyhedral mesh was used with 5 boundary layers near the pipe wall to achieve *y+* value below 1. A mesh independence stud has been carried out to ensure a mesh-independent solution.

Figure 2. Polyhedral mesh of CFD domain.

3. MULTI-CHANNEL MODEL

Prantoni M, et al. [9] have developed a method for the identification of open cells and closed cells. As shown in Fig.3, the trap cells was identified by two indices (i, j), as each open cell (orange cells) has an even sum of the indices, while the closed cells (black cells) have an

odd sum of the indices. According to the notation shown in Fig.3, the governing flow equation are defined as mass (Eq.1) and momentum (Eq.2) balance [9]:

$$\frac{d}{dx}\left(\rho_{i,j}u_{i,j}\right) = -(-1)^{i+j}\frac{1}{d_h}\,\rho_{i,j}\left(v_{i,j} + w_{i,j} + v_{i+1,j} + w_{i,j+1}\right) \qquad (1)$$

$$\frac{d}{dx}\left(\rho_{i,j}\,u_{i,j}^2\right) = -\frac{d}{dx}\left(p_{i,j}\right) - F\frac{\mu}{d^2}u_{i,j} \qquad (2)$$

where u_{ij} is the velocity in the (i,j) channel, p_{ij} is the pressure drop in the (i,j) channel, v_{ij} and w_{ij} are the filtration velocities trough the vertical and horizontal filter walls, ρ_{ij} is the gas density in the (i,j) channel evaluated trough the ideal gas low ($\rho_{ij}=p_{ij}/(R\,T)$ where R is the specific gas constant), μ_{ij} is the gas dynamic viscosity, F arise from the laminar theory in a square pipe [22] and it is equal to *28.454*, d_h is the cell hydraulic diameter and x is the axial coordinate varying from 0 (at the entrance from the filter) to L at the exit of the filter.

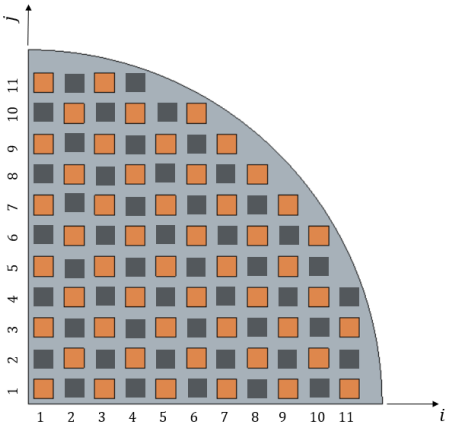

Figure 3. Cell index scheme.

In order to account for the pressure drop variation across the porous wall, the Darcy's law was used to determine the filtrations velocities that arises in Eq.1:

$$v_{i,j} = \frac{k}{\mu\, s}\left(p_{i,j} - p_{i-1,j}\right) \qquad (3)$$

$$w_{i,j} = \frac{k}{\mu\, s}\left(p_{i,j} - p_{i,j-1}\right) \qquad (4)$$

$$v_{i+1,j} = \frac{k}{\mu\, s}\left(p_{i,j} - p_{i+1,j}\right) \qquad (5)$$

$$v_{i,j+1} = \frac{k}{\mu\, s}\left(p_{i,j} - p_{i,j+1}\right) \qquad (6)$$

Substituting Eq.s.3-6 in Eq.1, and considering the ideal gas law, is it possible to define the following system of equations:

$$\frac{d}{dx}\left(p_{i,j}u_{i,j}\right) = -\frac{k}{d_h\,\mu\,s}\,p_{i,j}\left[\left(p_{i,j}-p_{i-1,j}\right)+\left(p_{i,j}-p_{i,j-1}\right)+\left(p_{i,j}-p_{i+1,j}\right)+\left(p_{i,j}-p_{i,j+1}\right)\right] \quad (7)$$

$$\frac{1}{R\,T}\frac{d}{dx}\left(p_{i,j}\,u_{i,j}^2\right) = -\frac{d}{dx}\left(p_{i,j}\right) - F\,\frac{\mu}{d_h^2}u_{i,j} \quad (8)$$

According to Prantoni M, et al. [9], the boundary conditions for the system use the known velocity entering in the inlet channel, zero velocity at the end of the inlet channel and beginning of the outlet channel, and a known pressure at the end of the outlet channel:

Inlet channels (*i* + *j* = even)

$$u_{i,j}(x=0) = U_{i,j} \quad (9)$$

$$u_{i,j}(x=L) = 0 \quad (10)$$

Outlet channels (*i* + *j* = odd)

$$u_{i,j}(x=0) = 0 \quad (11)$$

$$p_{i,j}(x=L) = p_{out} \quad (12)$$

where $U_{i,j}$ is the mean axial velocity at the entrance of the inlet channel (i,j), and p_{out} is the pressure at the exit of the outlet channel.

Eq.s.7-12 were solved through Matlab [23] and a boundary value problem solver '*bvp5c(…)*' has been used. The solver is a finite difference code that implements the four-stage Lobotto 3°a formula [24]. The CFD coupling methodology was explained in the next section.

4. COUPLING CFD AND MULTI-CHANNEL MODEL

The CFD and the Multi-Channel models were coupled through the front faces of the inlet channels (Fig. 4), and an iteration procedure was used to obtain a converged solution in both domains (see Fig.5).

As Prantoni M, et al. [9] demonstrated, Fig.6 shows the solution algorithm for the coupling between Star-CCM+ [21] and Matlab [23]. The procedure consists of:

1) setup CFD simulation with the pressure values at the inlet cells with an initial guess value.

2) Run the CFD simulation until convergence.

3) Extract the mean cross-sectional velocity entering each channel (Ui,j).

4) Use these velocities as inlet boundary conditions defined in Eq.9 for solving the boundary value problem using Matlab. The pressure pout defined in Eq.12 is setup as ambient pressure.

5) Extract the pressure at the entrance of each inlet channel from Matlab solution.

6) Update the outlet pressure condition of each entrance face of the inlet channels in the CFD simulation.

7) Repeat n times the steps 2) to 6) until the differences in backpressure is less than 10-6.

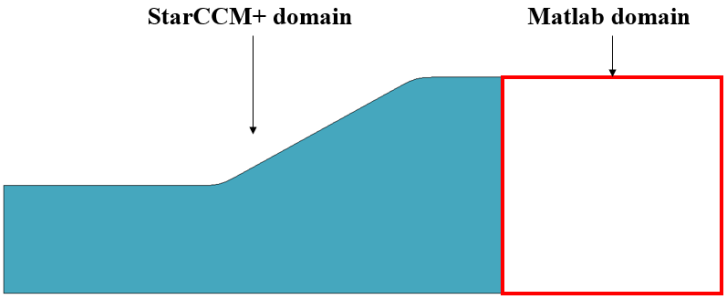

Figure 4. Computational domain in StarCCM+ and Matlab.

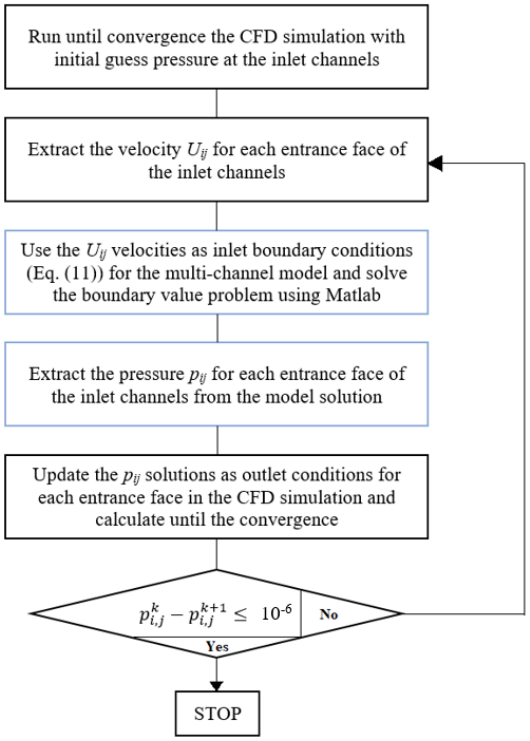

Figure 5. Algorithm.

5. RESULTS

For Matlab [23] numerical resolution the following filter properties have been considered:

- Filter length: $L=0.125\ m$
- Porous media permeability: k=5.5 10^{-3} m^2
- Hydraulic dyameter: $d=0.0014\ m$
- Pressure outlet: $p_{out}=0\ Pa$

Fig. 6 shows the last results of the iterative process. In particular, the velocity and the pressure range on a longitudinal section of the entire pipe is shown. It can be seen how the geometry of the pipe influences the fluid dynamics of the system. In fact, the areas of interface with the filter that are closest to the axis undergo a greater impact by the fluid, generating an overpressure around them, while the areas further away from the axis are little affected by the violence of the fluid impact. In Fig. 6 the velocities and pressures in the open cells are also shown. As it is easy to notice, the cells that undergo a higher input velocity are those halfway between the central units and those farthest from the axis.

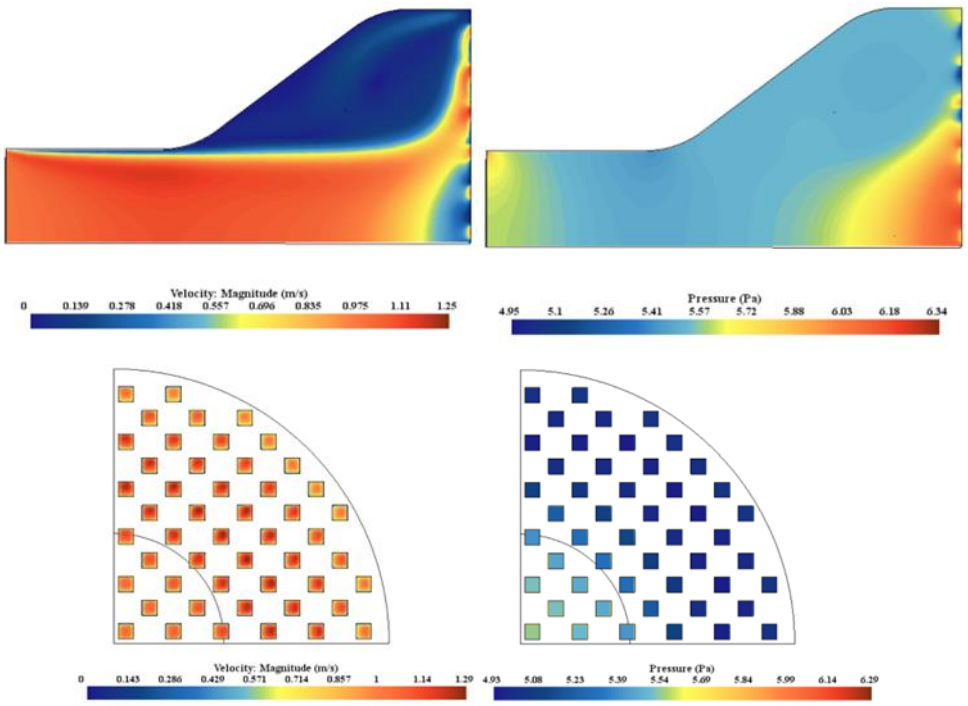

Figure 6. Velocity contour and relative pressure contour on longitudinal and frontal section.

It is however interesting to note that the pressure is not constant upstream of the filter and the geometric configuration influences the entire fluid dynamics as also demonstrated by Prantoni M, et al. [9]. To better visualize the areas where vortices were formed, a convolution integral on the velocity field has been shown in Fig. 7.

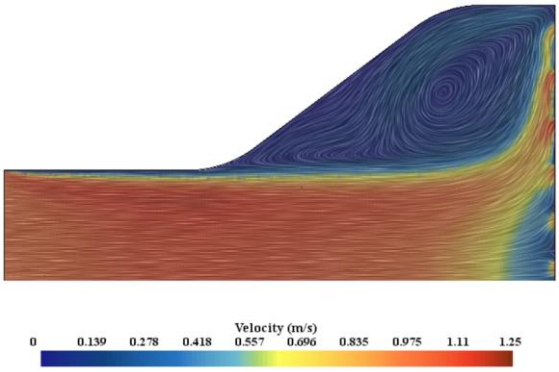

Figure 7. Velocity integral convolution for vortex visualization.

6. CONCLUSION

In this manuscript an alternative method for solving a fluid dynamics problem has been proposed. In particular, the influence of a wall-flow particulate filter it was studied on the fluid dynamics upstream of it. The conformation of the filter forces the fluid to pass through the small cells. This can lead into a numerical problem when one takes into account the real filters with a very high number of cells per mm^2 as it is necessary to create meshes that from large become very small. It is possible to get rid of this problem if the computational domains are separated: the fluid dynamic part upstream of the filter was solved through a classic CFD; the fluid dynamic part in the filter was solved externally by solving the equations that characterize the filter. The numerical coupling between the two different domains was carried out through an iterative procedure, which derives the input velocity to the filter cells from the CFD calculation and uses this as boundary conditions of the boundary value problem in the filter domain to derive the new pressure to be imposed in the outlet sections of the CFD domain. The results show that upstream of the filter the pressure distribution is not uniform. This means that the engine that pushes the exhaust fumes has to do more work to expel them.

The focus of the presented study was to demonstrate a software coupling methodology. The hypotheses made have a big weight on the final result:

- It was assumed that the relative pressure downstream of the filter was known (set equal to zero), but this value does not conform to reality. The actual conditions deviate from reality and this has an impact on the filter itself which must be taken into account.
- The soot accumulation or an initial soot layer in contact with the filter walls was not considered: this modifies the porous media permeability which will no be longer a continuous medium, but will be formed by layers of different material.

- A constant temperature has been assumed but, in reality, the temperature changes during the process and will result in changes in density, mass flow and pressure. This influence will be further explored in future works.

APPENDIX A

The standard *k*- ω model is an empirical model based on model transport equations for the turbulent kinetic energy, *k*, and the specific dissipation rate, ω. These quantities are obtained from the following transport equations:

$$\frac{\partial}{\partial x_i}(\rho k u_i) = \frac{\partial}{\partial x_j}\left(\Gamma_k \frac{\partial k}{\partial x_j}\right) + G_k - Y_k \quad (1.A)$$

$$\frac{\partial}{\partial x_i}(\rho \omega u_i) = \frac{\partial}{\partial x_j}\left(\Gamma_\omega \frac{\partial \omega}{\partial x_j}\right) + G_\omega - Y_\omega \quad (2.A)$$

Where ρ is the fluid density, u_i is the fluid velocity component, G_k and G_ω represents the generation of k and ω, Γ_k and Γ_ω represent the effective diffusivity ok *k* and ω, Y_k and Y_ω represent the dissipation ok *k* and ω due to turbulence. More information can be found in the literature for a better understanding.

7. REFERENCES

[1] R. Niessner, 'The many faces of soot: Characterization of soot nanoparticles produced by engines,' Angewandte Chemie - International Edition, vol. 53, no. 46, pp. 12366–12379, Nov. 2014, doi: 10.1002/anie.201402812.

[2] J. Tollefson, 'Soot a major contributor to climate change,' Nature, Jan. 2013, doi: 10.1038/nature.2013.12225.

[3] A. J. Torregrosa, J. R. Serrano, F. J. Arnau, and P. Piqueras, 'A fluid dynamic model for unsteady compressible flow in wall-flow diesel particulate filters,' Energy, vol. 36, no. 1, pp. 671–684, 2011, doi: 10.1016/j.energy.2010.09.047.

[4] C. Fragassa, 'Electric City Buses with Modular Platform: A Design Proposition for Sustainable Mobility,' Smart Innovation, Systems and Technologies, vol. 68, pp. 789–800, 2017, doi: 10.1007/978-3-319-57078-5_74.

[5] G. Minak, C. Fragassa, and F. V. de Camargo, 'A Brief Review on Determinant Aspects in Energy Efficient Solar Car Design and Manufacturing,' Smart Innovation, Systems and Technologies, vol. 68, pp. 847–856, 2017, doi: 10.1007/978-3-319-57078-5_79.

[6] G. Minak, T. M. Brugo, C. Fragassa, A. Pavlovic, F. v. de Camargo, and N. Zavatta, 'Structural Design and Manufacturing of a Cruiser Class Solar Vehicle,' JoVE (Journal of Visualized Experiments), vol. 2019, no. 143, p. e58525, Jan. 2019, doi: 10.3791/58525.

[7] M. Prantoni et al., 'Modelling Pressure Losses in Gasoline Particulate Filters in High Flow Regimes and Temperatures,' 2019.

[8] E. J. Bissett, 'Mathematical Model Of The Thermal Regeneration Of A Wall-Flow Monolith Diesel Particulate Filter,' 1984.

[9] M. Prantoni, S. Aleksandrova, H. Medina, and S. Benjamin, 'Multi-channel modelling approach for particulate filters,' Results in Engineering, vol. 5, Mar. 2020, doi: 10.1016/j.rineng.2019.100077.

[10] S. Aleksandrova et al., ‘Turbulent Flow Pressure Losses in Gasoline Particulate Filters,’ Source: SAE International Journal of Engines, vol. 12, no. 4, pp. 455–470, 2019, doi: 10.2307/26897923.

[11] G. Koltsakis, O. Haralampous, C. Depcik, and J. C. Ragone, ‘Catalyzed diesel particulate filter modeling,’ Reviews in Chemical Engineering, vol. 29, no. 1, pp.161,Feb.2013,doi:10.1515/REVCE20120008/MACHINEREADABLECITATION/RIS.

[12] S. Yang, C. Deng, Y. Gao, and Y. He, ‘Diesel particulate filter design simulation: A review:,’ http://dx.doi.org/10.1177/1687814016637328, vol. 8, no. 3, pp. 1–14, Mar. 2016, doi: 10.1177/1687814016637328.

[13] A. N. Impiombato, C. Biserni, M. Milani, and L. Montorsi, ‘Prediction Capabilities of a One-dimensional Wall-flow Particulate Filter Model,’ J. Appl. Comput. Mech, vol. 8, no. 1, pp. 245–259, 2022, doi: 10.22055/JACM.2021.38708.3270.

[14] U. Lantermann and D. Hänel, ‘Particle Monte Carlo and lattice-Boltzmann methods for simulations of gas–particle flows,’ Computers & Fluids, vol. 36, no. 2, pp. 407–422, Feb. 2007, doi: 10.1016/J.COMPFLUID.2005.10.005.

[15] L. P. Wang, C. Peng, Z. Guo, and Z. Yu, ‘Lattice Boltzmann simulation of particle-laden turbulent channel flow,’ Computers & Fluids, vol. 124, pp. 226–236, Jan. 2016, doi: 10.1016/J.COMPFLUID.2015.07.008.

[16] C. Rettinger and U. Rüde, ‘A coupled lattice Boltzmann method and discrete element method for discrete particle simulations of particulate flows,’Computers&Fluids, vol.172, pp. 706–719, Aug. 2018, doi:10.1016/J.COMPFLUID.2018.01.023.

[17] H. Wei, J. S. Chen, and M. Hillman, ‘A stabilized nodally integrated meshfree formulation for fully coupled hydro-mechanical analysis of fluid-saturated porous media,’ Computers & Fluids, vol. 141, pp. 105–115, Dec. 2016, doi: 10.1016/J.COMPFLUID.2015.11.002.

[18] J. Huang, F. Xiao, H. Dong, and X. Yin, ‘Diffusion tortuosity in complex porous media from pore-scale numerical simulations,’ Computers & Fluids, vol. 183, pp. 66–74, Apr. 2019, doi: 10.1016/J.COMPFLUID.2019.03.018.

[19] K. Yamamoto, S. Satake, H. Yamashita, N. Takada, and M. Misawa, ‘Fluid simulation and X-ray CT images for soot deposition in a diesel filter,’ Eur. Phys. J. Special Topics, vol. 171, pp. 205–212, 2009, doi: 10.1140/epjst/e2009-01030-x.

[20] D. WILCOX, ‘A half century historical review of the k-omega model,’ Jan. 1991, doi: 10.2514/6.1991-615.

[21] Siemens Digital Industries Software, ‘Simcenter STAR-CCM+, version 2021.1.1.’ 2021.

[22] N. C. Markatos, ‘Transport processes in chemically reacting flow systems,’ International Journal of Heat and Mass Transfer, vol. 33, no. 5, p. 1039, May 1990, doi: 10.1016/0017-9310(90)90087-B.

[23] MATLAB, ‘R2022a.’ The MathWorks Inc. Natick, Massachusetts, 2022.

[24] L. Shampine, J. Kierzenka, and L. F. Shampine, ‘A BVP solver that controls residual and error A BVP Solver that Controls Residual and Error 1,’ European Society of Computational Methods in Sciences and Engineering (ESCMSE) Journalof Numerical Analysis, Industrial and Applied Mathematics (JNAIAM), vol. 3, no. 2, pp. 27–41, 2008, Accessed: Mar. 29, 2022. [Online]. Available: https://www.researchgate.net/publication/228748602

Biographies

Luca Montorsi received the master's degree in mechanical engineering from University of Modena and Reggio Emilia in 1999, and the philosophy of doctorate degree in Materials Engineering from University of Modena and Reggio Emilia in 2003, respectively. He is currently working as an Full Professor at the Department of Sciences and Methods for Engineering, Faculty of Engineering, University of Modena and Reggio Emilia. His research areas include Fluid Power and System for Energy Conversion and Environment. He has been serving as a reviewer for many highly-respected journals.